Chapter 4
Microfluidic Technology for Single-Cell Manipulation

Weifei Zhang, Nan Li and Jin-Ming Lin

Abstract Single-cell analysis has attracted much attention in the field of biological and biomedical study owing to the heterogeneity among individual cells. This poses significant challenges to conventional bulk assays which would mask rare but important information owing to the assumption of average behavior. To avoid the interference of useless cells and obtain the single cells in the trial of genomics, proteomics, metabonomics, and single-cell behavior study, various cell manipulation techniques have been developed for single-cell research. In this chapter, we introduce the principles of droplet generation and single-cell encapsulation and review the latest achievements of cell manipulation technique by categorizing externally applied manipulation forces: microstructures, electrical, optical, magnetic, acoustic, and mechanical. This chapter will also introduce our latest work and provide important references and ideas for the development of droplet microfluidic-based single-cell manipulation.

Keyword Microfluidics · Droplet · Single-cell encapsulation · Cell manipulation · Single-cell lysis

4.1 Introduction

The cell as the fundamental unit of life has been extensively studied for expressions of genes, proteins, and metabolites [1–3]. In conventional methods for biochemical analysis, samples are usually collected from a large number of cells treated with certain stimulus in order to obtain sufficient molecules for meeting the sensitivity of the detection instrument. Thus, the results are averaged over the number of cells. However, it has been frequently found that the behaviors of individual cells are not identical even with the same type cells cultured in the same microenvironment. As a result, the bulk assays usually mask some rare but crucial information and even

W. Zhang · N. Li · J.-M. Lin (✉)
Department of Chemistry, Tsinghua University, Beijing 100084, People's Republic of China
e-mail: jmlin@mail.tsinghua.edu.cn

J.-M. Lin (ed.), *Microfluidics for Single-Cell Analysis*,
Integrated Analytical Systems, https://doi.org/10.1007/978-981-32-9729-6_4

cause some misleading interpretations [4–6]. Therefore, to characterize the cell-to-cell differences and discern cellular subpopulations, single-cell analysis becomes necessary [7, 8].

To accurately describe and elucidate the heterogeneities among single cells, systems with high throughput and sensitivity are needed. These two requirements have driven the development of microfluidic system, where an aqueous flow is segmented into individual droplets within an immiscible carrier fluid (often a mineral or fluorinated oil) to encapsulate single cell [9–11]. Such systems offer several key advantages for single-cell analysis. The first is parallelization: multiple identical microreactor units can be formed in a short time, and parallel processing can easily be achieved, allowing large data sets to be acquired efficiently. The second is miniaturization: droplet reactors have small dimensions, in the range from subnanoliter to picoliter level, making it possible for the single-cell analysis. The third is compartmentalization: droplets formed in the microfluidic channels can be used as independent units for manipulation [12–14]. Owing to these advantages, recently droplet microfluidic technology has been applied to various fields of single-cell research, such as signal response, nucleic acid analysis [15–18], protein analysis [19–21], and metabolite analysis [22, 23].

In this chapter, we will introduce the recent developments and outstanding achievements of droplet microfluidic technology in single-cell manipulation. Based on the study procedure, the main content is divided into four parts: droplet generation, single-cell encapsulation, cell manipulation, and single-cell lysis. This chapter will also discuss the challenges and prospect of droplet microfluidics in single-cell analysis and provide important reference for the development of biomedical research and application.

4.2 Droplet Generation

Although the variety of methods have been developed to drive the dispersed phase into the continuous phase and form the droplets, the fluid behavior can be characterized through some crucial dimensionless numbers, which are calculated via the parameters of the fluid properties, flow conditions, and geometric features. The significant physical parameters, which determine droplet formation, can be characterized through calculation of the capillary number $Ca = \mu U/\gamma$, where μ (Pa s) and U (m s^{-1}) are the viscosity and velocity of the continuous phase, and γ (N m^{-1}) is the surface tension of the droplet interface. With the increase of Ca value, the various flow regimes are defined as the squeezing, dripping, and jetting, which are depicted in Fig. 4.1. For a more detailed discussion of these three regimes, some brilliant publications or reviews are recommended to the readers [24, 25]. In addition, there are also some other dimensionless number which are related to the droplet breakup under a high flow rate or a large-dimensional geometry. For example, Weber number (We) is used to report the relative importance of inertia with respect to interfacial tension; Bond number (Bo) reflects the relative

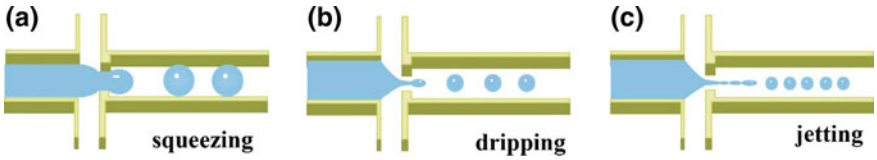

Fig. 4.1 Three regimes for droplet generation, squeezing, dripping, and jetting with an increase of capillary number

importance of gravitational forces with reference to interfacial tension; and Reynolds number (*Re*) indicates the relative importance of inertial forces with respect to viscous forces.

4.2.1 Droplet Generation by Passive Methods

In passive methods driven by the external pumps, two immiscible fluids (dispersed phase and continuous phase) meet at a junction, which determines interface deformation and droplet breakup, as shown in Fig. 4.2a [22]. According to the

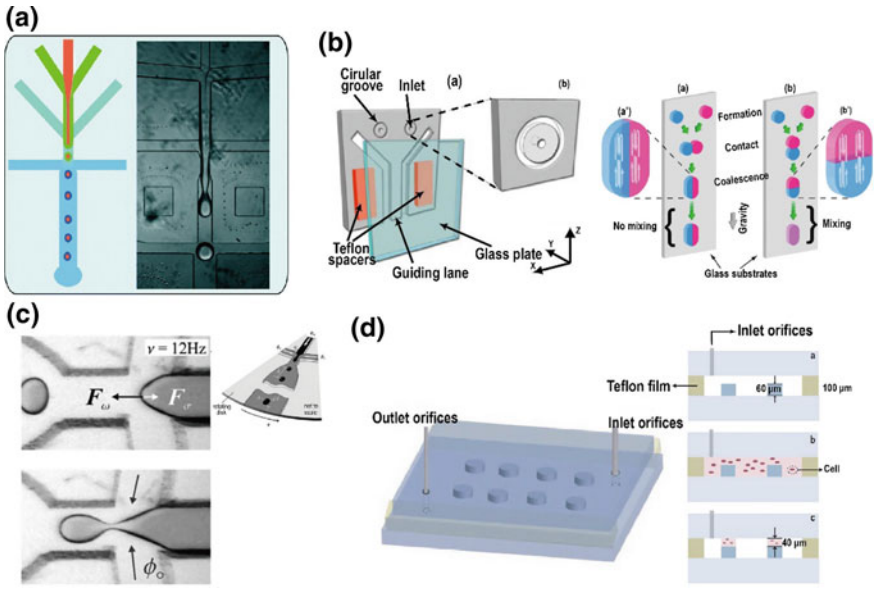

Fig. 4.2 Droplet generation by passive method. **a** Droplets can be generated by two immiscible fluids, and the droplet size can be adjusted by changing the ratio of oil and water flow rates, which were controlled through a syringe- or pressure-driven pump [22]. **b** Droplets were produced by a circular groove surrounded inlet [26]. **c** Droplets were generated by centripetal forces using a rotating microfluidic device [27]. **d** Droplets were generated through protrudent circular plot arrays based on surface tension [28]

complex geometrical design of the microchannel junction, the droplet formation can be classified into coflow, cross-flow, and flow-focusing categories. Besides, Lin's laboratory also reported an approach to generate monodispersed droplets on a microfluidic chip without using a carrier liquid, which employed a circular groove surrounded inlet for the droplet formation, as shown in Fig. 4.2b [26]. However, exert pumps are not the only way to produce pressure gradients for droplet generation. Häberle et al. have presented a method which used a rotating microfluidic device to generate the centripetal force for droplet generation in a traditional flow-focusing geometry, as shown in Fig. 4.2c [27]. Li et al. developed a microdevice with protrudent circular plot arrays for the formation of nanoliter droplets by surface tension without any additional equipment, as shown in Fig. 4.2d [28].

4.2.1.1 Coflow

In the coflow category, the two immiscible phases flow in a set of coaxial microchannels in the same direction. The dispersed fluid flows into an inner channel, and the continuous phase is introduced into an outer concentric channel as shown in Fig. 4.3a. Fischer et al. [29] were the first to report the coflow experimental setup, which consisted of a cylindrical glass capillary tube nested within a square glass tube. By ensuring that the inner dimension of the square tube was the same as the outer diameter of the cylindrical tube, a good alignment to form a coaxial geometry was achieved. Thorough experimental data provided by the authors indicated that the fluid properties and flow rates were two important factors to determine the droplet size. Increasing the continuous flow velocity reduced the droplet size owing to a higher shear stress, while increasing the dispersed flow rate resulted in an increase of droplet size, as a larger volume of dispersed fluid entered a droplet before breakup. In comparison with the velocity, the viscosity of the two phases had rather weak effects on the droplet size.

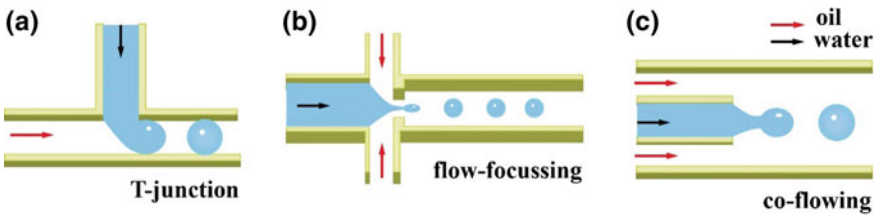

Fig. 4.3 Scheme of three geometrical designs of the microchannel junction: coflowing, cross-flowing, and flow-focusing

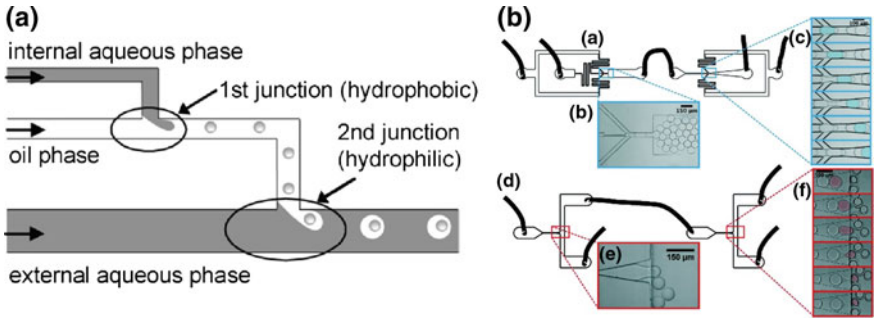

Fig. 4.4 Common methods for generating multilayered droplets. **a** A double T-junction cross structure for double emulsions [32]. **b** A double flow-focusing structure for double emulsions [35]

4.2.1.2 Cross-Flow

Cross-flow category is achieved by using angled microchannels. T-junction is a common structure, in which dispersed and continuous phases flow through orthogonal channels at a cross junction, as shown in Fig. 4.3b. Thorsen was the first to use T-junction to generate droplets [30]. In this configuration, the main channel is introduced with the continuous phase and the side channel is infused with the dispersed phase. These two immiscible phases are intersected at focused zone in a perpendicular way to generate droplets under the regulation of surface tension and shear stress. The two asymmetric forces from side channel and main channel, together with the surface tension, break the dispersed phase to independent droplets [31]. The droplet formation process can be summarized as dropping, spraying, and deformation. The droplet size and formation rate can be effectively adjusted by changing the flow velocity, channel size, and liquid viscosity. Additionally, multi-emulsions can be generated through reasonable use of multiple T-junction (Fig. 4.4a) [32]. However, it should be noted, the asymmetry force in droplet generation process will have a great influence on the cells encapsulated in droplets, and thus, T-junction had better be used in other aspects instead of cell analysis.

In addition, some other modified geometry designs are also developed for various purposes. For instance, a "K-junction" type was reported to provide an exit channel for the waste [33]. And a "V-junction" type was designed for a high degree of operational flexibility [34].

4.2.1.3 Flow-Focusing

The flow-focusing geometry is composed of three channels, one main channel and two symmetric side channels. These channels are focused on a narrow region connecting the downstream channel, and two immiscible phases flow coaxially through this narrow region, which has the function of shear-focusing and thus

contributes to uniform droplet generation, as shown in Fig. 4.3c. Currently, this method has the ability to make relatively small droplets and the droplet-generation process is closely related to the size of the narrow region. This design has an advantage that the dispersed phase in focused zone will only suffer from the driving force. Since the side channels are symmetrical, force from other directions would be counteracted, which will reduce the interference to cells and keep the droplets stable. Similarly, the size of the droplet is determined by the flow ratio of the two phases. The larger the velocity of the continuous phase is, the smaller and faster the generated droplet is. Besides the size of the focusing region, the viscosity of the liquid also influences the formation and size of droplets. Similar to the multiple T-junction, the application of multiple flow-focusing structures can also obtain multilayered droplets (Fig. 4.4b) [35].

4.2.2 Droplet Generation by Active Methods

As for active methods, the droplet generation can occur on-demand with the application of an active, short-duration external forced. According to the categories of energy sources, active method-based droplet generation can be classified into electrical, magnetic, thermal, and mechanical methods.

4.2.2.1 Electrical Method

Electrical source can be used to modulate the size of droplets. Our group reported a series of work that utilized the piezoelectric inkjet to generate drop-on-demand monodispersed droplets with the volume of picoliter level. This method was easy to control and the droplet size can be regulated by adjusting the piezoelectric actuation including driving voltage and pulse width. As an ideal generator of droplets, inkjet was coupled to various analytical instruments, such as mass spectrometry and capillary electrophoresis. Chen et al. integrated drop-on-demand inkjet cell printing and probe electrospray ionization mass spectrometry (PESI-MS) to study the single-cell lipid. The single-cell-containing droplets were generated via inkjet sampling, followed by precisely dripping onto a tungsten-made electrospray ionization needle for immediate spray under a high-voltage electric field, as shown in Fig. 4.5a [36]. Zhang et al. combined the inkjet printing system with capillary electrophoresis (CE) to investigate the separation of cells, which validated the feasibility of inkjet printing for mammalian cells to achieve the drop-on-demand and convenient sampling into capillary [37]. Further, they developed a novel and flexible online digital polymerase chain reaction (dPCR) system, which consisted of an inkjet for generating the droplets, a coiled fused-silica capillary for thermal cycling, and a laser-induced fluorescence detector (LIFD) for positive droplet counting. Upon inkjet printing, monodisperse droplets were continuously generated in the oil phase and then introduced into the capillary in the form of a stable

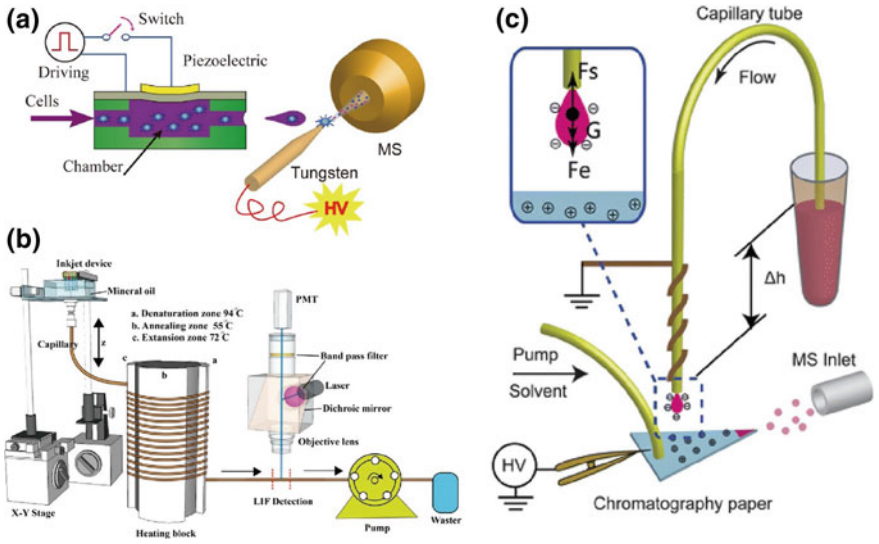

Fig. 4.5 Droplet generation by electrical methods. **a** Inkjet printing-based droplet single-cell MS analysis [36]. **b** Inkjet printing-based droplet PCR analysis [15]. **c** Droplet generation *via* gravity and electrostatic attraction for ESI-MS analysis [39]

dispersion. The droplets containing one or zero molecules of target DNA passed through the helical capillary that was attached to a cylindrical thermal cycler for PCR amplification, resulting in the generation of fluorescence for the DNA-positive droplet, as shown in Fig. 4.5b [15]. Korenaga et al. also utilized the inkjet printing technique as a sample introduction method to pattern cells onto ITO glass substrate for MALDI-MS detection, allowing the sample diameter with the range of a few hundred micrometers [38]. Apart from inkjet for the droplet formation, Liu et al. generated submicroliter droplets via gravity and electrostatic attraction and provided a proof-of-principle experiment to show the utilization of paper-based electrospray ionization mass spectrometry (ESI-MS) in the online analysis of the generated droplets, as shown in Fig. 4.5c [39]. Further, based on this mechanism and protocol of droplet formation, they established a homemade microdialysis module for ESI-MS [40]. Besides, Link et al. incorporated electrodes with a constant direct current voltage into the flow-focusing device, as shown in Fig. 4.6a, where the water flow acted as a conductor, and the oil stream served as an insulator. This led to the accumulation of charge at the droplet interface, and thus, electrical field force also played an important part in controlling the droplet size apart from the interfacial tension and viscous force [41]. The higher the voltage was, the smaller the droplet size was. Additionally, an alternating current can also be applied to generate the droplets via the electrowetting-on-dielectric (EWOD) effect, because the contact angle between the conductive liquid flow and the channel could be reduced by exerting an electrical field.

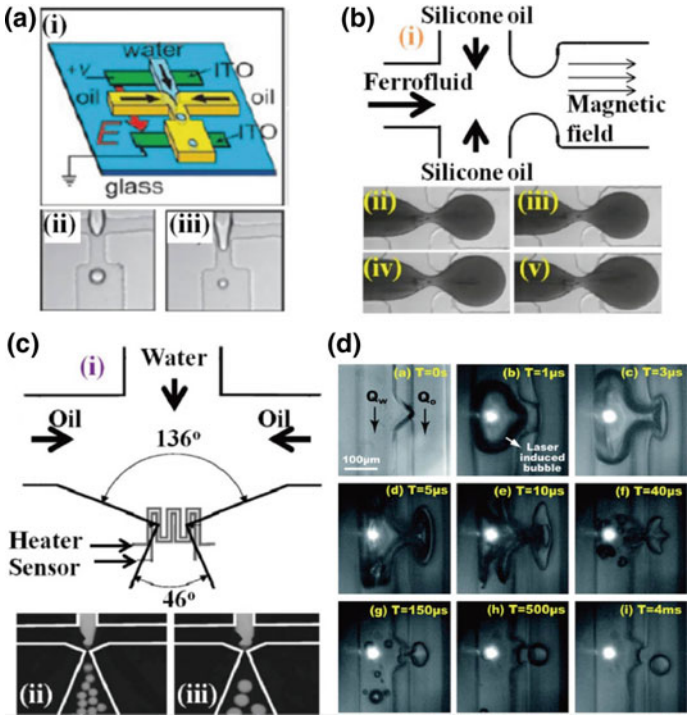

Fig. 4.6 Droplet generation by active methods. **a** Droplet generation by applying a direct current voltage [41]. **b** Droplet generation by applying a magnetic field [42]. **c** Droplet generation by thermal method [43]. **d** Droplet generation by optical method [45]

4.2.2.2 Magnetic Method

The droplet formation can also be achieved through the non-contact, magnetic control, such as ferrofluids which can be suspended in either aqueous or oily carrier liquid. Nguyen et al. reported a method to use an aqueous ferrofluid as the dispersed phase, and the magnetic force could drag the ferrofluid tip forward until the droplet formation, Fig. 4.6b [42]. A magnetic bond number, Bm, indicating the relative strength of the magnetic force to interfacial tension, is used to characterize the droplet behavior.

4.2.2.3 Thermal Method

The thermal source can be used to control the droplet generation owing to the dependency of Ca on the temperature, because the fluid properties such as viscosity and interfacial tension can vary with the temperature. The whole device or junction can be heated, and thermal resource can also be introduced through a localized laser

irradiation. A previous study has report that the droplet generation was modulated by integrating a microheater and a temperature sensor into a flow-focusing device, as shown in Fig. 4.6c [43]. The fluid viscosity and interfacial tension were normalized as the functions of the temperature, and the results suggested that the droplet size could be well controlled by the temperature.

4.2.2.4 Optical Method

Optical method has been used to generate picoliter-level droplet, even achieving to create femtoliter-volume droplets on-demand in nanofluidic channels [44]. Park et al. used a focused pulsed laser to produce a cavitating microbubble in the neighborhood of a T-junction position, generating picoliter-level monodispersed W/O droplets during a few milliseconds with a rate of up to 10 kHz (Fig. 4.6d) [45].

4.3 Single-Cell Encapsulation

Since the delivery of cells to the droplet-generation nozzle is a random process with a Poisson distribution, accurate control of the number of cells in each droplet is challenging [46]. Usually, the cell suspension is largely diluted for the requirement of single-cell encapsulation, which leads to a large number of empty droplets [47]. Consequently, a variety of methods to remove droplets containing no cells have been developed. Viovy et al. were the first to report a purely hydrodynamic approach to confine the single cells into a picoliter-level droplet prior to spontaneous self-sorting based on the sizes. A cell-triggered Rayleigh–Plateau instability in a flow-focusing structure helps the single cells to be encapsulated in the droplets. Two extra hydrodynamic mechanisms, lateral drift of deformable objects in a shear flow and sterically driven dispersion in a compressional flow, realized the self-sorting, as shown in Fig. 4.7a [48]. This method was demonstrated to have a significant improvement in single-cell encapsulation and the sorting rate could reach 70–80%. Further, Chen et al. presented a passive separation strategy, which used a droplet jetting generator and a deterministic lateral displacement (DLD) size-sorting channel to encapsulate single cells into aqueous droplets and separated cell-encapsulated droplets from empty droplets for subsequent assays. Due to the cell-triggered Rayleigh–Plateau instability in the process of droplet jetting, large cell-containing droplets (diameter 25 μm) and small empty droplets (diameter 14 μm) were generated. Then, size-based sorting was performed inside the DLD micropillar channel, where the critical dimension for separation is defined by geometric design [49]. Furthermore, to avoid the restrictions of cell stochastic encapsulation, one cell should be present whenever a droplet is produced. This can be achieved by regulating cells in the direction of flow with the same frequency when they enter the microfluidic nozzle. Toner et al. have reported a method that allowed cells self-organizing into two evenly spaced streams and 80% single-cell

encapsulation efficiency could be obtained when a high-density suspension of cells was forced to travel rapidly through a high aspect-ratio microchannel, as shown in Fig. 4.7b [50]. Kemna et al. used a Dean-coupled inertial ordering of cells in a simple curved continuous microchannel to achieve single-cell encapsulation in picoliter droplets with an efficiency of up to 77%, as shown in Fig. 4.7c [51]. Further, another method was developed by using a short pinched flow channel composed of contracting and expanding chambers to conduct inertial focusing along the channel center, which quantified the single-cell encapsulation efficiency >55%, as shown in Fig. 4.7d [52].

Although a variety of studies have been reported to circumvent the block of low single-cell encapsulation efficiency, yet the optimal encapsulation efficiency was less than 80%. Thus, more studies are suggested to further address this issue from the point of technical development.

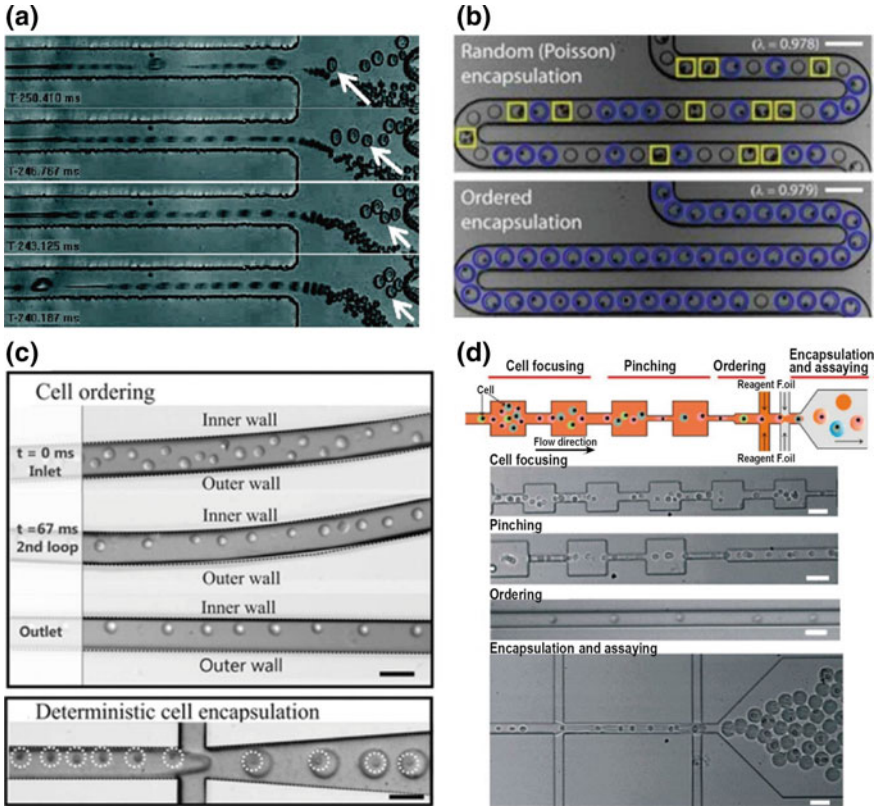

Fig. 4.7 Methods for improving the single-cell encapsulation efficiency. **a** Size-based droplet sorting after single-cell encapsulation by a hydrodynamic approach [48]. **b–d** Inertial flow-based cell spacing and single-cell encapsulation via (**b**) a high aspect-ratio straight channel [50]. **c** A curved channel [51]. **d** A short pinched flow channel [52]

4.4 Cell Manipulation

With the development of microfluidic chip, the cell manipulation technology coupled with microfluidic techniques becomes a promising tool for single-cell-level manipulation. To reduce the interference of useless cells and obtain the single pure target cell for the single-cell analysis, such as genetic analysis, protein analysis, and metabolism analysis, a variety of single-cell manipulation techniques have been developed. These manipulation techniques can be divided into passive and active methods [53]. Passive methods use rationally designed microfluidic structures to control cell positions, for instance, pinched flow [54] and deterministic lateral displacement [55]. Active methods use actuators to manipulate cells and are classified depending on the externally applied manipulation forces: electrical [56], optical [57], magnetic [58], acoustic [59], and mechanical. The advantages and drawbacks of each cell manipulation technique were described in this part.

4.4.1 Microstructures Manipulation

The precise design of microstructures including microwells, microbarriers, and microtraps can be used in biological study, such as cell capture, pairing, patterning, and subsequent cell culture [60–62]. These approaches have the advantages on high-throughput, high-efficient, and ease of operation and have been extensively used in single-cell systems. Sarioglu et al. [63] developed a Cluster-Chip that contained a series of triangular pillars, and these unique geometries were exploited to differentiate CTC clusters from single cells in blood. This strategy realized specific and label-free isolation of CTC clusters from patients with various cancer types, and then achieved the release of CTC clusters, allowing for downstream molecular and functional assays. Lecault et al. [64] developed a microfluidic platform containing thousands of nanoliter-scale chambers for longer-term mammalian cell culture. This platform enabled in situ immunostaining and recovery of viable cells, and was applied to high-throughput investigation of hematopoietic stem cell proliferation at the single-cell level.

4.4.2 Electrical Manipulation

Electrokinetic forces originating from the electric field have been widely applied to microfluidic cell manipulation owing to the feasibility of integrating microelectrodes in microfluidic chips [65]. Generally, electrokinetic manipulations were classified into three categories: electrophoresis [66], dielectrophoresis [67], and electroosmosis [68], and these techniques have all been realized on microfluidic chips.

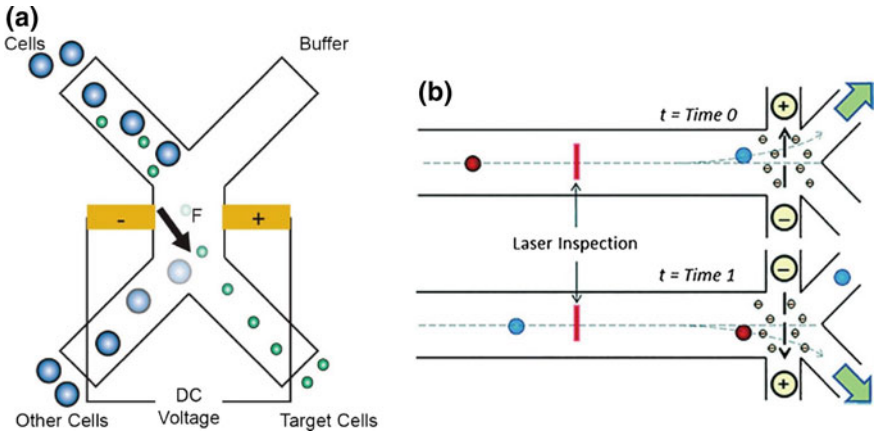

Fig. 4.8 Schematics of electrical manipulation techniques for single cells. **a** Electrophoresis manipulation. Cells with negative charge move toward the positive electrode. **b** Electroosmotic flow manipulation. Negatively charged ions moving toward the positive electrode induce secondary fluid movements for cell manipulation [70]

4.4.2.1 Electrophoresis

Generally, most cells membrane were negative at neutral pH. Thus, suspended cells with negative charge will move toward a positive electrode direction under the application of a constant electric field [69]. In a solution, the cells obtain a velocity resulted from a force balance, where the dominant forces exerting on the cell are the Coulomb and drag forces. For the separation of different cell types, it is necessary for the cells to have different charge or size [65], and this separation mode is called electrophoresis (EP) (Fig. 4.8a) [70]. Takahashi et al. [71] have developed a device which enabled two laminar flow streams to converge at the center. Cells are introduced in one stream and imaged thirty times per second as they pass the convergence point. At the position where the electrodes were connected between the two streams with an applied voltage, certain specific cell was recognized depending on the phase contrast and fluorescence, and the electrophoretic force causes the cell to jump from one stream to the other. Likewise, Guo et al. [72] sorted single-cell-containing droplets into different streams through a pulsed electric field. However, it should be noted, it is not a good alternative to use electrophoresis to separate the heterogeneous cell suspensions, because the specificity of electrophoretic migration is not obvious between cells [65, 73].

4.4.2.2 Dielectrophoresis

In comparison with electrophoresis, dielectrophoresis is a more popular method for cell manipulation owing to the higher specificity in dielectric properties among

various cell types. There are also some other advantages, such as harmless to the cell, pre-treatment free, high precision and easy to manipulate an individual cell. And this term "dielectrophoresis" was first presented by Pohl in 1951, who used small plastic particles suspended in insulating dielectric liquids to perform significant early experiments and found that the particles could move in response to the application of a non-uniform alternating current or direct current electric field [74]. Currently, dielectrophoresis has been developed in single-cell manipulation field by acting a non-uniform electric field upon a neutral object. The magnitude of DEP force is determined by the size, shape, electrical property of the single cell, and the electric field gradient. For a spherical cell, it could be assumed that the electric field (E) does not change significantly over the cell surface. As a result, the time-averaged dielectrophoresis force $\langle F_{\mathrm{DEP}} \rangle$ could be calculated according to the following equation.

$$\langle F_{\mathrm{DEP}} \rangle = 2\pi r^3 \varepsilon_{\mathrm{m}} Re[f_{\mathrm{CM}}(\omega)] \nabla |E|^2$$

Here, r was the radius of cells, ε_{m} was the permittivity of the culture medium, and $\nabla|E|^2$ described the intensity of the electric field at each point, regardless of the direction. And an important term, real part of Clausius–Mossotti (CM) factor ($Re[f_{\mathrm{CM}}(\omega)]$) determined the direction of the dielectrophoresis force and controlled the direction of cell motion, which was defined based on the dielectric properties of the cells and culture medium, and was a function of the applied frequency. The Clausius–Mossotti factor can be described as a function of the medium and the particle complex permittivities as follows:

$$f_{\mathrm{CM}}(\omega) = \frac{\varepsilon_{\mathrm{c}}^*(\omega) - \varepsilon_{\mathrm{m}}^*(\omega)}{\varepsilon_{\mathrm{c}}^*(\omega) + 2\varepsilon_{\mathrm{m}}^*(\omega)}$$

where $\varepsilon_{\mathrm{c}}^*(\omega)$ and $\varepsilon_{\mathrm{m}}^*(\omega)$ represent complex permittivity of cells and culture medium, respectively. And complex permittivity is dependent on permittivity (ε), conductivity (σ), and angular frequency ($\omega = 2\pi f$) of the applied electric field, which can be described as follows:

$$\varepsilon_{\mathrm{c\,or\,m}}^* = \varepsilon_0 \varepsilon_{\mathrm{c\,or\,m}} - j\frac{\sigma_{\mathrm{c\,or\,m}}}{2\pi f}$$

For mammalian cells, dielectric properties can be formulated by the protoplast model. CM factor for live cells can be rewritten as the following equation:

$$f_{\mathrm{CM}}(\omega) = -\frac{\omega^2(\tau_{\mathrm{m}}\tau_{\mathrm{c}}^* - \tau_{\mathrm{c}}\tau_{\mathrm{m}}) + j\omega(\tau_{\mathrm{m}}^* - \tau_{\mathrm{m}} - \tau_{\mathrm{c}}^*) - 1}{\omega^2(2\tau_{\mathrm{m}}\tau_{\mathrm{c}}^* + \tau_{\mathrm{c}}\tau_{\mathrm{m}}^*) - j\omega(\tau_{\mathrm{m}}^* + 2\tau_{\mathrm{m}} + \tau_{\mathrm{c}}^*) - 2}$$

where $\tau_{\mathrm{c}}^* = c_{\mathrm{m}} r/\sigma_{\mathrm{c}}$ and $\tau_{\mathrm{c}} = \varepsilon_{\mathrm{c}}/\sigma_{\mathrm{c}}$ are time constants for cells. c_{m} is membrane capacitance. σ_{c} and ε_{c} are conductivity and permittivity of cells, respectively. In addition, $\tau_{\mathrm{m}}^* = c_{\mathrm{m}} r/\sigma_{\mathrm{m}}$ and $\tau_{\mathrm{m}} = \varepsilon_{\mathrm{m}}/\sigma_{\mathrm{m}}$ are time constants for medium. σ_{c} and ε_{c}

represent conductivity and permittivity of medium, respectively. The value of f_{CM} factor is limited within −0.5 to 1 and changed with the frequency. When the value is <0, the cells are less polarizable than the culture medium and suffered from a negative dielectrophoresis force, which drives the cell to move toward the direction of weak electric field intensity. When the value >0, the cell will move toward the strong electric field under the manipulation of a positive dielectrophoresis force. Based on the theory of dielectrophoresis, a large number of device have been designed for single-cell manipulation including cell separation [75], trapping/capturing and release [76].

The electric field gradient can be determined by different electrode shapes. Consequently, various electrode shapes have been designed for cells or particles manipulation, such as ring electrode Fig. 4.9a and b [77], quadrupole electrode Fig. 4.9c, d [78]. Further, actuation electrodes have been integrated into microfluidic chip for the dielectrophoresis manipulation of single cell. Park used such an integrated chip to detect the trapping single cell through the impedance method, as shown in Fig. 4.10 [79]. For high-efficient single-cell trapping and analysis, an integrated microfluidic chip containing a microwell array inside was reported [80].

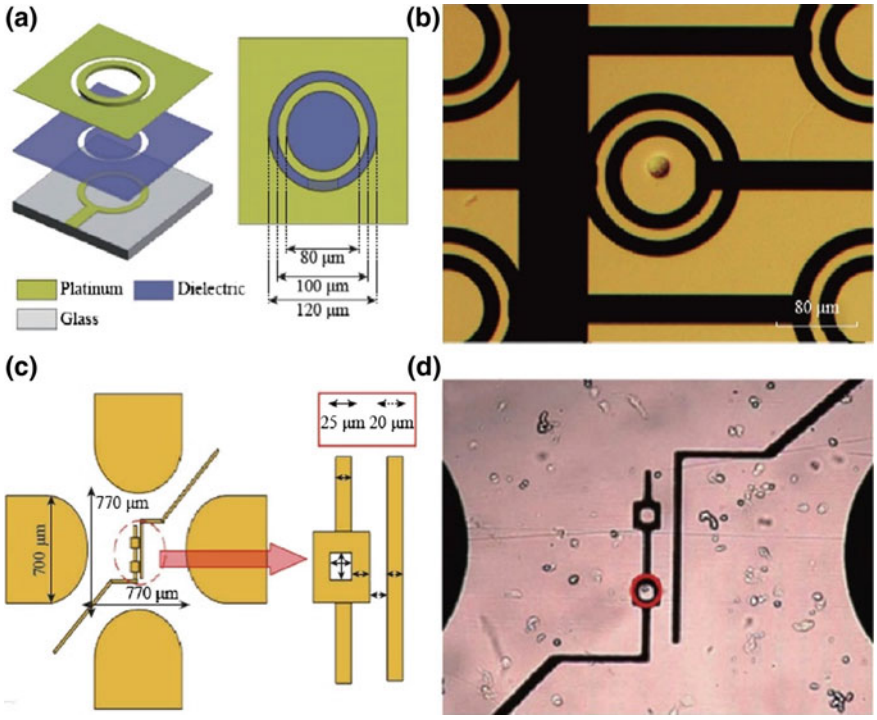

Fig. 4.9 Different electrodes applied with voltage to generate non-uniform electric field for single-cell manipulation. **a**, **b** Ring electrode [77]. **c**, **d** Quadrupole electrode [78]

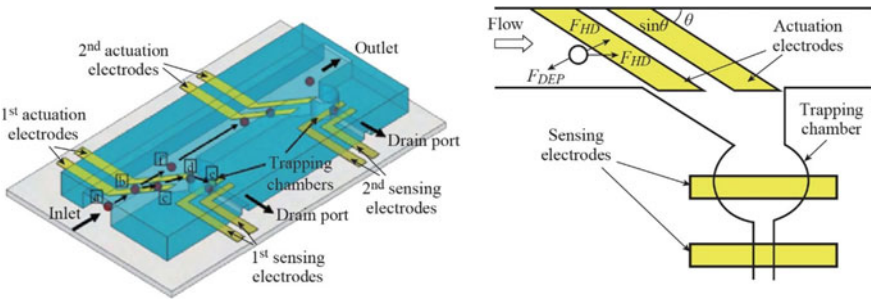

Fig. 4.10 Schematic of the microfluidic chip and illustration of the forces acted on the particle [79]

4.4.2.3 Electroosmotic Flow

Similar to preceding discussion about electrophoresis and dielectrophoresis, electroosmotic-based separation was also caused by an applied electric field. However, they have different phenomenological process. Electroosmotic flow (EOF) refers to fluid motion with the direction of inducing solvated ion transport under an electric field (Fig. 4.8b) [70]. Dittrich and Schwille have reported a sorting microchip that leveraged a pump to drive primary flow to create electroosmotic flow, and this pressure-driven method enabled a fast and stable flow rate, allowing a high-throughput cell sorting [81]. The advantage of electroosmotic flow typically lies in the precise control of volumetric flow through various channels occupying the same microfluidic device. However, to use the electroosmotic flow to manipulate the single cell, the electrodes have to be fabricated on the microfluidic chip, leading to complicated operation. What is worse, it is harmful for cells to be exposed to electric fields, resulting in a decrease of cell viability. Despite all these defects, this method has the ability to precisely control small volumes-based cell separation.

4.4.3 Optical Manipulation

A few decades ago, a focused laser was found that could propel microparticles in a liquid, and this was the origination of optical manipulation [82]. In the following, these researchers used a tightly focused laser to achieve stable trapping, forming the foundation of contemporary “optical tweezers” [83]. Optical tweezers are significant tools and have been used to manipulate single cells on microfluidic chips, which rely on a tightly focused laser beam to manipulate single cells with little damage to the cell behaviors. In an optical process, single cells are easily trapped at the focal point of laser beams, which enables the isolation of single cells with great convenience (Fig. 4.11a) [84]. Similar to the dielectrophoresis, the behavior of cells

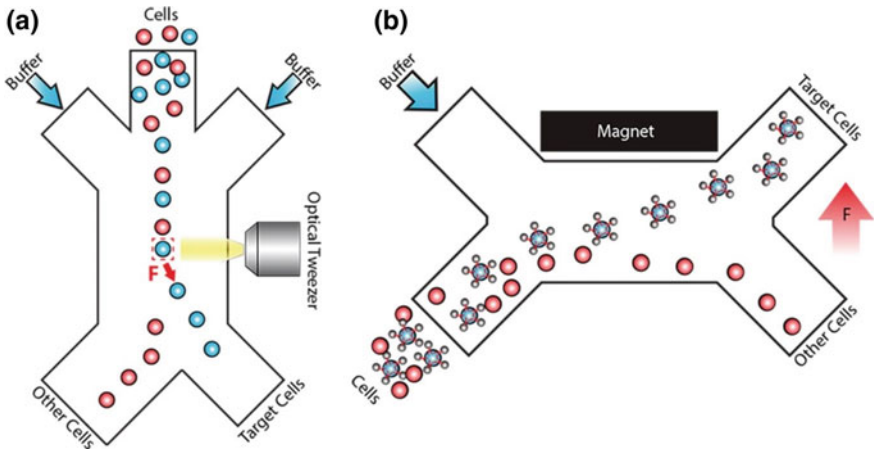

Fig. 4.11 Schematics of single-cell manipulation via optical and magnetic method. **a** The cells are repositioned toward the appropriate outlet under the manipulation of the optical tweezer. **b** The target cells labeled with magnetic beads are manipulated to move toward a distinct outlet compared to the nontarget cells [84]

is determined by their refractive index compared to the surrounding fluid. The cells will migrate toward the region of highest light intensity when the cells' refractive index is higher than that of the surrounding fluid and vice versa. More detailed descriptions can be found elsewhere [85, 86]. Osellame et al. integrated a femtosecond laser to an optofluidic device for optical trapping and stretching of single red blood cells, which provided accurate alignment between the optical and fluidic components, as shown in Fig. 4.12a [87]. Kim et al. integrated optical tweezers to microfluidic chip as a generic single-cell manipulation tool for handling small cell population sorting with high accuracy, as shown in Fig. 4.12b [88]. Kovac et al. have fabricated a microwell array on a microfluidic chip, where the mammalian cells could load. Then, target cells were selected by microscopy and were levitated from their wells into a flow field for collection by using the scattering force form a focused infrared laser, as shown in Fig. 4.12c [89].

4.4.4 Magnetic Manipulation

Magnetic manipulation methods are required to conjugate the magnetic particles to cells via a cell-specific antibody on the magnetic particle. Subsequently, these specific cells can be separated by passing the sample through a microfluidic device exerted a magnetic field or magnetized surface (Fig. 4.11b) [84]. In comparison with the electrical cell manipulation, which requires electrodes in contact with the cell suspension and may damage the cell viability owing to the electrochemical reactions at the electrode fluid interface, magnetic manipulation enables simplicity

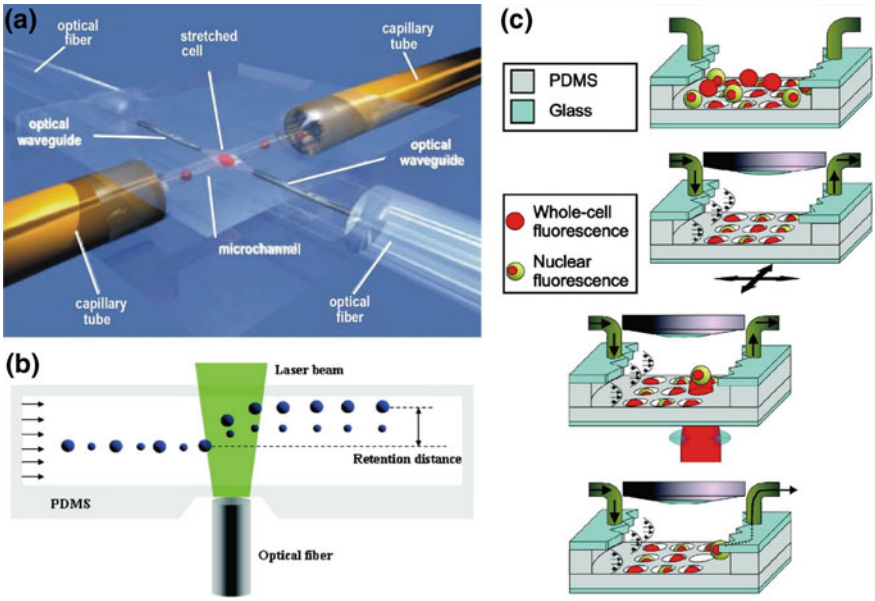

Fig. 4.12 Single-cell manipulation by optical methods. Various structures of optical manipulation devices. **a** Single cells are trapped at the focal point of laser beams [87]. **b** Sing cells are separated depending on the size of cells by optical force [88]. **c** Single cells trapped in a microwell are pushed out of the microwell by using an optical manipulation technique [89]

and capacity to separate via action at a distance is a significant advantage compared to. Wang et al. have reported that they isolated CTCs from whole blood through treating whole blood with magnetic nanoparticles that were functionalized with anti-EpCAM antibody [90]. Liu et al. developed a simple and straightforward approach, which used NIH 3T3 cells incubated in a medium containing magnetic fibers as assay samples, to fabricate magnetic nanofiber segments for cell manipulation. The result showed that cells can be conveniently manipulated with a magnet, as shown in Fig. 4.13 [91].

4.4.5 Acoustic Manipulation

Recently, acoustic manipulation has attracted much attention owing to the negligible impact on cell viability [92]. The mechanism of acoustic manipulation was that an acoustically generated pressure wave can induce cell movement, and several subdistinctions of acoustic cell manipulation was classified depending on the wave type: bulk standing waves, standing surface acoustic waves, and traveling waves.

Bulk standing waves can be created in microfluidic channels when the applied wavelength matches the spatial channel dimension. Consequently, along the wave's

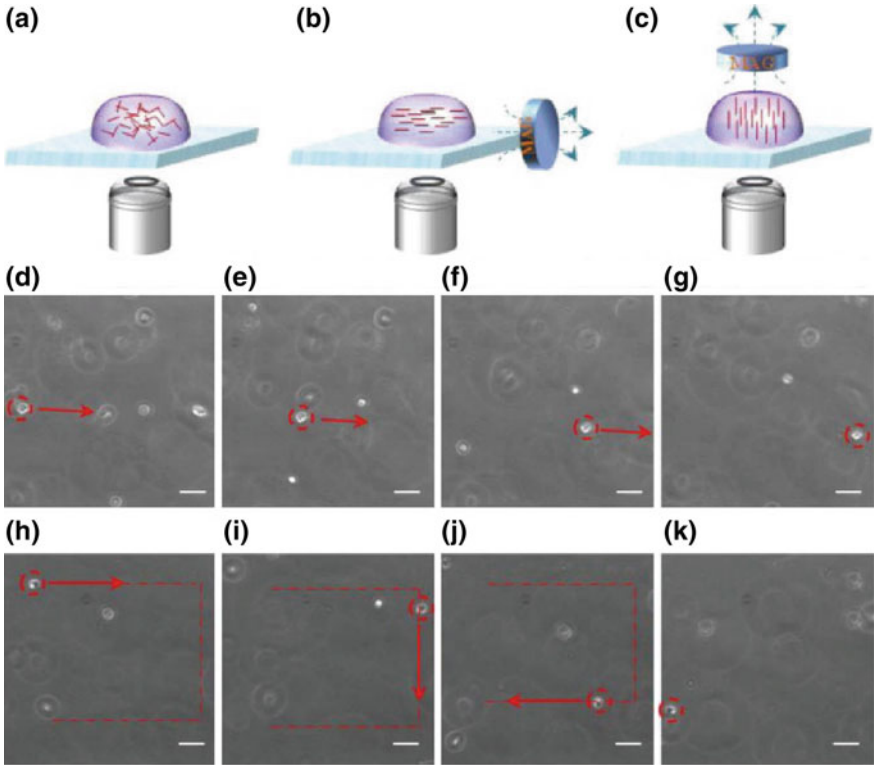

Fig. 4.13 **a–c** Schematic of magnetic particle doped nanofiber segments in water drops on a glass slide. **d–k** Showing cell movement path, controlled by an external magnetic field. The scale bar is 20 μm [91]

path, two distinct regions appear across the channel, where the first is termed a node without a pressure fluctuation and the second is termed an antinode with a fluctuating pressure alternating between a minimum and maximum, as shown in Fig. 4.14a [70]. Cells will have a response to the standing wave according to their acoustic contrast factor when they flow through the channel. And the acoustic contrast factor is determined by cell density and compressibility relative to the surrounding medium. Cells having a positive acoustic contrast factor will move toward the node, while cells with negative acoustic contrast factors will be driven to the antinodes. Thus, the single cells can be divided into different outlets. Grenvall et al. [93] integrated a two-dimensional acoustic focusing region on a microfluidic chip, where the cells could be separated to five different outlets based on the size of the cells, as shown in Fig. 4.15. This device has capacity to sort white blood cells of high purity and viability.

Standing surface acoustic waves (SSAW) are formed along the bottom of a microfluidic channel using interdigital transducers (IDTs) that are mounted on a microfluidic chip in the form of a piezoelectric substrate. The modes of acoustic

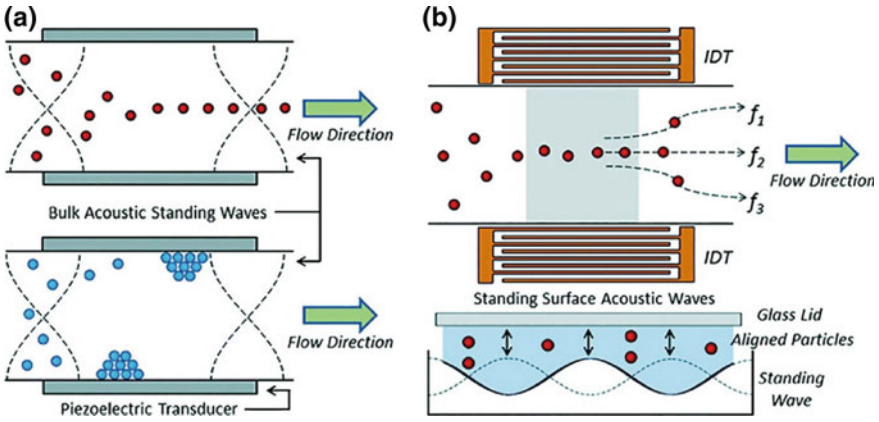

Fig. 4.14 Schematics of cell manipulation by acoustic methods. **a** Acoustic manipulation via bulk standing waves, where the cells' acoustic contrast factor determines their migration to the node or antinode. **b** Acoustic manipulation via standing surface waves, where the acoustic waves are generated by interdigitated electrodes position cells at distinct streamlines [70]

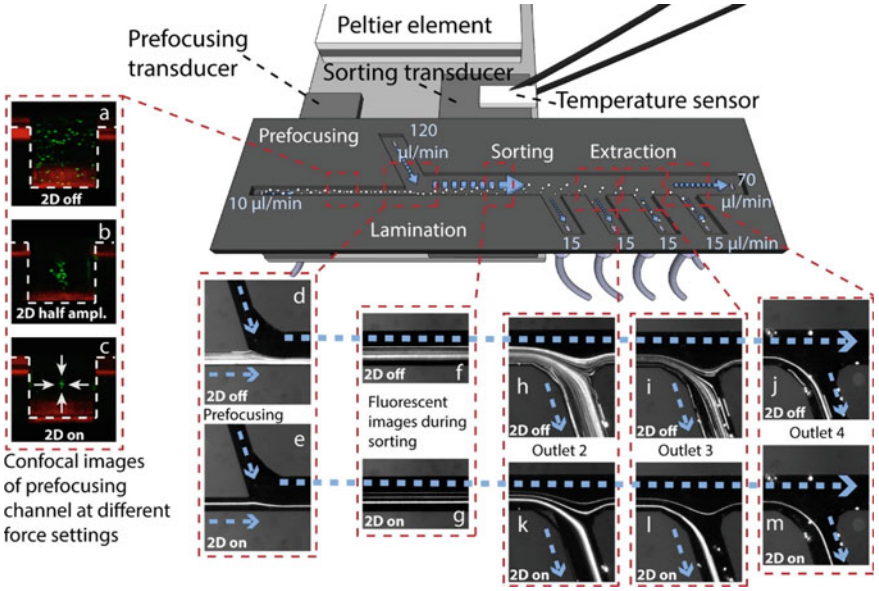

Fig. 4.15 A schematic of on-chip cell manipulation with two-dimensional acoustically focused region [93]

wave in the fluid varied from a transverse wave to a longitudinal wave, allowing the generation of a pressure node. The cells are separated into different streamlines and outlets through these acoustic waves generated by the cross-shaped electrodes, as

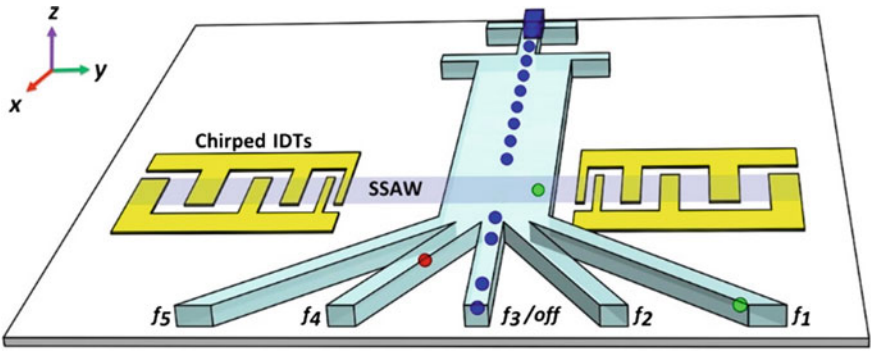

Fig. 4.16 A schematic of droplet-sorting device according to the principle of standing surface acoustic wave [94]

shown in Fig. 4.14b [70]. Since the standing surface acoustic wave has the ability to move the cells or particles into different deflection based on the different contrast factors in the fluid, it is a flexible approach for single-cell manipulation in comparison with bulk standing waves. Li et al. [94] have reported to use a standing surface acoustic waves-based chip to manipulate the W/O droplets into five different outlets, as shown in Fig. 4.16.

Although most of the acoustic-based cell manipulation is based on standing waves, traveling acoustic wave is still an alternative for single-cell manipulation. Contrary to the standing wave which usually needs to match the wavelength of the acoustic wave with the width of the microfluidic channel, the traveling wave breaks this restrict without the limitation of wavelength. Schmid et al. applied a fluorescence-induced traveling wave to sort cells into three channels and the cell sorting rate was increased by a factor of 10 in comparison with the use of a standing surface acoustic wave [95].

Similar to electrically based cell sorting, it is necessary for the acoustic method to integrate a sensor on the chip, leading to a complex manufacturing and an increased cost.

4.4.6 Mechanical Manipulation

Mechanical methods use mechanical forces, such as gravity, hydrodynamic, and suction to manipulate cells. Rettig et al. designed different microwell dimension arrays for large-scale single-cell trapping [96]. They investigated some parameters, including microwell diameter, microwell depth, and settle time, to maximize single-cell occupancy for two cell types. There are also some other structures for

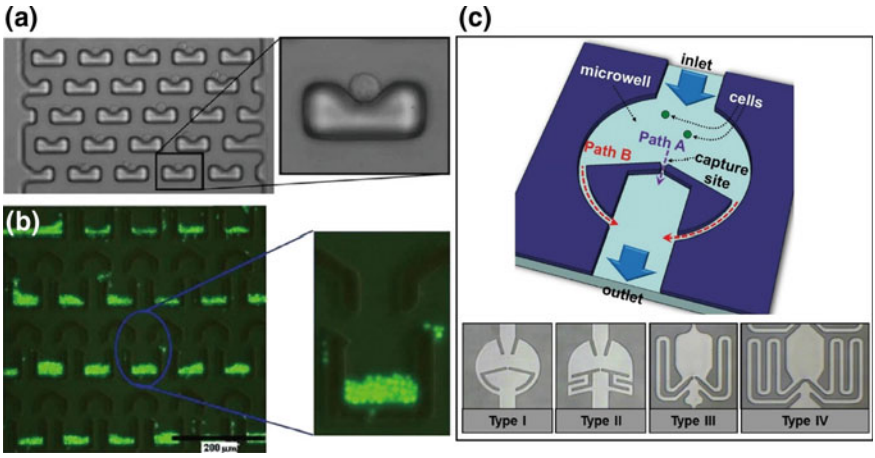

Fig. 4.17 Different shapes for cells trapping. **a** Cells capture by a U-shaped structure [97]. **b** Cells captured in U-shape with Y-shaped fluidic guide [98]. **c** Four kinds of different structure for cells capture [99]

cell manipulation base on hydrodynamic. For example, a physical U-shape hydrodynamic trapping structures array has been developed for single-cell trapping and culture, as shown in Fig. 4.17a [97]. Chen et al. designed another structure for cells capture, where the first layer consists of spacers to create a small gap between the upper layer and glass and the second layer is a U-shaped compartment with sharp corners at the fore-end. And a Y-shaped fluidic guide structures are designed on the top of each U-shaped capture structures, shown in Fig. 4.17b [98]. Furthermore, there was another highly efficient single-cell capture device using hydrodynamic guiding structures, and four types of cell capture module were designed and tested for optimal structure. The results showed that the capturing efficient of this single-cell capture chip was more than 80% and the structures for single-cell trapping were shown in Fig. 4.17c [99].

Despite the continuous improvement of the structures, however, those designs only can be used for one or several kinds of cells owing to its manipulation principle based on both geometric size of cells and capture structures. Thus, the method leveraged suction for cell manipulation was presented. A micromanipulation method for single prokaryotic cells extracting was proposed, shown in Fig. 4.18 [100]. Similarly, another design depending on the method of suction was presented by Anis and coauthors. They integrated a picoliter pump into a robotic manipulation system, where this picoliter pump could automatically select and transfer single target cells onto analysis locations. Using this method, they successfully accomplished single-cell manipulation with Barrett's esophagus cells [101].

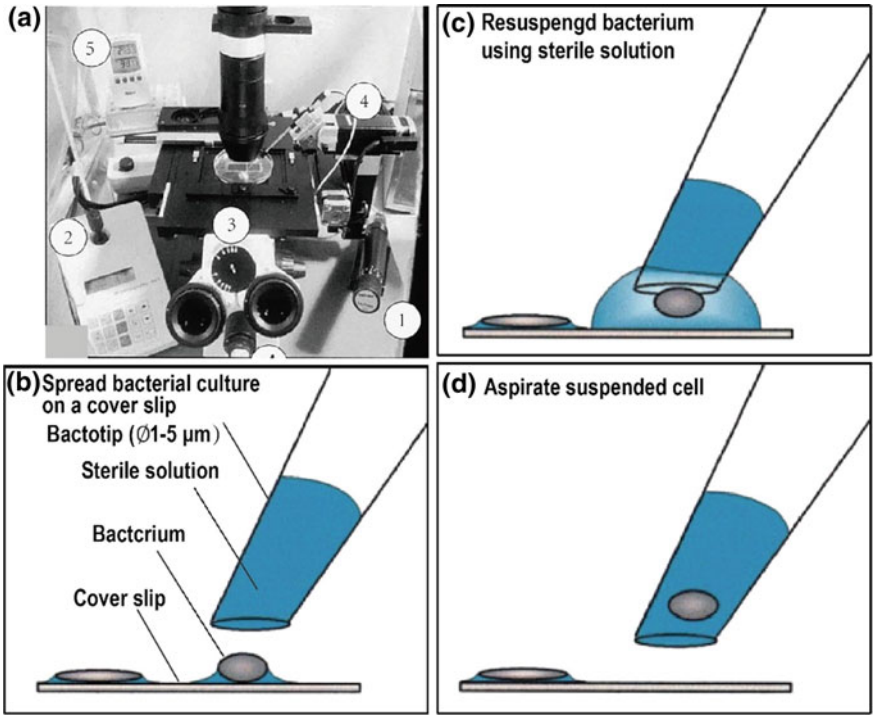

Fig. 4.18 Workstation and schematics of procedure for isolating the single bacterial cell. **a** Aspirate the spread cells through a Bactotip. **b** Spread bacterial culture on a cover slip. **c** Suspend bacterium using sterile solution. **d** Aspirate suspended cell [100]

4.5 Single-Cell Lysis on Microfluidics

Once a target single cell is captured, the biomolecules in the cells are required to be extracted for the following assay. To extract the molecule inside the cells, the cell plasma membrane has to be disrupted. Conventional strategies for membrane disruption can be classified into two aspects, non-detergent and detergent-based. Non-detergent-based methods include mechanical agitation, liquid homogenization, temperature cycling, and sonication. However, these methods are suitable for many cells in suspension or larger tissue samples rather than single-cell analysis. Detergent-based cell lysis is much milder and quicker approach in comparison with mechanical, sonication, and freeze–thaw cell lysis, and can be scaled down for single cells. Detergents play a role in disrupting interactions between lipids and proteins, and can be characterized depending on the nature of their hydrophobic tail and hydrophilic head. For the selection of detergent, general rules are useful; nonionic or zwitterionic detergents are less denaturing compared with ionic detergents, and therefore, they are used when the native protein structure or function need to be maintained. To maintain the native structure and expression of the

biomolecules, a frequent goal of cell lysis is to minimize their alteration as much as possible. That is to say, the lysis approach must be both gentle and rapid. For single-cell analysis, some commonly used methods, such as sonication, freeze–thaw, and detergent may exist their disadvantages: excessive heat generation, long protocols, and arduous implementation. However, the development of microfluidic technology has enabled new cell lysis approaches, specifically suited for single cells.

4.5.1 Mechanical Lysis

Mechanical force induced by shear, compression, collision with sharp features, and so on has been used to puncture the cell membranes. Kim et al. [102] fabricated a microfluidic chip with spatio-specific and reversible channel for the mechanical strain application and release, and this design was successfully applied to single-cell lysis. In this performance, channels were created via applied strain and a single cell was placed in the newly formed channel, subsequently, the strain was released and the channel was collapsed, the single cell was lysed via compression. However, it is a pity that this method required manual handling to put the single cells into the channels. Hoefemann et al. [103] proposed a single-cell lysis method using a continuous microfluidic flow, which can lyse the single cell in less than 20 ms with 100% efficiency. When the cells passed through an integrated heater, they were compressed against the channel ceiling owing to the generated bubbles, as shown in Fig. 4.19a. However, it should be noted that a following single-cell assay was not performed in this report. Consequently, we should consider some factors, such as lysate diffusion and compartmentalization before we used this method for the single-cell molecular analysis.

4.5.2 Thermal Lysis

Thermal lysis can be a good alternative when some additional reagent such as enzymatic or detergent may contaminate the intracellular biomolecules. However, as some biomolecules are heat-sensitive, careful consideration and precise control of the temperature is required. Consequently, it is rare for protein analysis to use thermal cell lysis. Instead, this method is frequently used for parallel, on-chip PCR analysis that requires additional temperature cycling. Gong et al. loaded a large number of single cells into on-chip wells and conducted cell lysis by heating the chip to 50 °C for 40 min, followed by DNA amplification through temperature cycle [104]. Besides, the lysis time is also another critical limitation for thermal lysis. Considering that the occurrence of thermal lysis generally needs a timescale of minutes, thus this technique is not suitable for monitoring intracellular signaling events which occur within seconds [105]. This reason explains that thermal lysis is

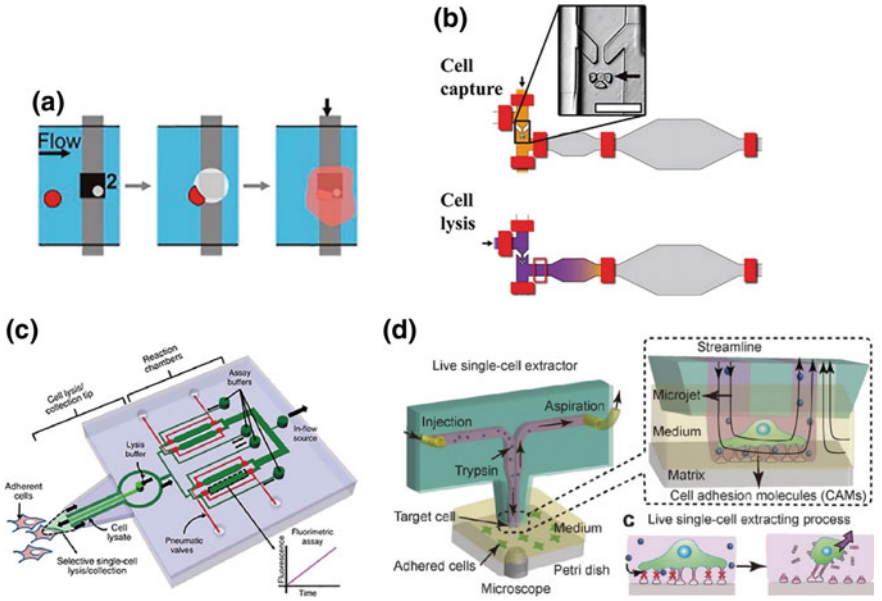

Fig. 4.19 Schematics of methods for single-cell lysis. **a** Single-cell lysis by mechanical methods. Single cells are lysed when passed through the bubble generated above the heater [103]. **b** Single-cell lysis by chemical methods. Lysis buffer is mixed with the single cell trapped in the chamber [106]. **c** A microfluidic device for single-cell lysis in adherent cell culture. The device tip is positioned at the single cell and a hydrodynamically focused lysis buffer selectively lyses the target cell [117]. **d** A microfluidic chip for live single-cell extraction, which can be used to study the single-cell detachment process

most frequently used for gene expression with the occurrence of several hours. In addition, thermal lysis has also been applied to some droplet microfluidic platforms for continuous single-cell PCR research.

4.5.3 Chemical Lysis

Chemical lysis has become a popular technique for single-cell lysis owing to its long history of application to bulk cellular analysis. The instruction of reagents can be regarded as a guide for selecting the appropriate lysing protocol for single cell. Many factors can determine the lysing speed, including the kind of detergent or enzyme being utilized, the concentration, and the contact efficiency. Ionic detergents such as sodium dodecyl sulfate have a fast lysis rate in comparison with nonionic detergents such as Triton X-100. However, the proteins will be denatured under the condition of ionic detergents. Generally speaking, the maximal contact efficiency is desirable for faster cell lysis, while it is challenged to perform this in

microfluidic systems, because molecular transport and mixing are dominated by diffusion in such a device where microscale flows typically occur in the viscous flow regime. Shi et al. [106] have reported a method that they used cell lysis buffer, which was brought into contact with cells strictly via diffusion, to lyse single cells isolated in microfluidic chambers. 20 min lysis buffer diffusion was allowed, and another 20 min was used for incubation. As mentioned above, the lysis time limits the study for faster occurring intracellular events. To overcome this obstacle, some additional installations, such as peristaltic pumps, syringe pumps, actuating valves (Fig. 4.19b), or manual pipet injections are applied to sequentially move reagents across cells for a thorough mixture [107–111]. Additionally, chemical lysis can be used for continuous single-cell analysis by simultaneously performing cell compartmentalization and lysis. DeKosky et al. [112] used a flow-focusing nozzle to encapsulate single lymphocytes in lithium dodecyl sulfate-containing droplets, and the lysis efficiency was reported to reach 100%. A large number of research about RNA sequencing [113, 114], PCR [113, 115], and single-cell enzyme activity [116] have been reported by using the droplets for single-cell compartmentalization and chemical lysis.

Despite the great progress of single-cell lysis, most of them require cells to be in suspension for the manipulation, making it difficult to correlate single-cell data with their native context such as intact tissue or adherent cultures. Some previous reports have suggested that cell surface receptor activation or protein modification would change upon removing from native context and these changes are challenged to be measured [105]. To circumvent this limitation, Sarkar et al. [117] presented a strategy that can selectively lyse a single cell and capture lysate in adherent status with a minimal dilution. In this microfluidic chip, an outflow of lysis buffer was produced at a device tip, and the lysis buffer is hydrodynamically confined to a small scale by a balanced surrounding inflow of lysis buffer, as shown in Fig. 4.19c. Similarly, Lin's laboratory [3] presented a live single-cell extractor (LSCE) for the study of adhered single cells on a cell culture dish based on laminar flow (Fig. 4.19d). The tip of the LSCE fabricated with PDMS was immersed perpendicularly into a Petri dish, where the adhered single cells were extracted in automated mode. A stable microjet of laminar flow occurred underneath the tip of the LSCE when the ratio of aspiration to injection was sufficiently high, allowing the extraction of adhered cells. Despite the low throughput and manual position, this method is unique in its ability to analyze single-cell protein activity in adherent cell culture.

4.5.4 Electrical Lysis

The bilayer of cell membrane suffers from reorientation and thermal phase transitions and new pores can be formed upon exposure to an electric field [118]. The formation of the pore is reversible when the electric field is mild (0.2–1 V) and the exposure time is short, which is termed electroporation and is frequently applied to

deliver therapeutic and genetic materials into cells [119]. On the contrary, the formation of the pore is permanent with strong electric fields or prolonged exposure, leading to an unbalanced osmotic pressure between the cytosol and the surrounding media, followed by the swell and rupture of the cells. Additionally, a high electric field can also cause rapid cell rupture [120]. Electrical cell lysis is preferred because it can be tuned for rapid cell lysis without denaturing target biomolecules. Another advantage is that the cell membrane or organelle membrane can be selectively ruptured owing to the difference between their membrane potential [121]. Young et al. designed a microfluidic device for electroosmotic flow positioning and electrical lysis of a single lymphoma cell with a success rate of 80%. And it takes approximately 60 s on average from cell injection to cell lysis [122]. Kim et al. loaded 95% 3600 wells with single cells by integrating microwell compartmentalization, DEP immobilization, and electrical cell lysis all on one chip. Under the condition of pressure-driven flow, reagent exchange was done rapidly in 30 s without perturbing the cell positioning [80]. The lysates can be confined by physically closing the wells through pressing a PDMS membrane on top of the wells. Subsequently, 100% of trapped cells were simultaneously lysed under a series of 30 V electrical pulses. Contrary to the thermal lysis or chemical lysis, electrical methods offer rapid cell lysis without the damage of an assay's target biomolecule and avoid potential target contamination. Nevertheless, electrical lysis is not free limitation because electrical lysis requires integration of electrodes and respective control systems on a microfluidic chip, causing a block to clinical application.

4.6 Conclusions and Perspective

Since the technological advances in amplification, sequencing, and microfluidics, the single-cell analysis becomes particularly exciting, and the single-cell research is believed to have a profound influence in cancer diagnosis, immunology, and stem cell research. Up to now, a number of single-cell manipulation techniques have been reported, especially for the droplet-based microfluidic. There is no doubt that innovative manipulation techniques have made great contributions to the field of single-cell analysis and will continue to play an important role. However, despite the great progress in single-cell manipulation, most of them still require further parameter optimization for standardization and commercialization. Moreover, the manipulation techniques should also fulfill some purposes, such as obtaining the target cell with high purity, high efficient, high throughput, low injury, and high precision. Besides, many studies ignored the influence from the cells' native tissue, leading to the cell's behavior change. To analyze the exact preclinical samples for current clinical trials, single-cell manipulation techniques need to be further developed for handling the cell in native context.

References

1. Zhang L, Vertes A (2018) Single-cell mass spectrometry approaches to explore cellular heterogeneity. Angew Chem Int Ed 57(17):4466–4477. https://doi.org/10.1002/anie.201709719
2. Altschuler SJ, Wu LF (2010) Cellular heterogeneity: do differences make a difference? Cell 141(4):559–563. https://doi.org/10.1016/j.cell.2010.04.033
3. Mao S, Zhang W, Huang Q, Khan M, Li H, Uchiyama K, Lin JM (2018) In situ scatheless cell detachment reveals correlation between adhesion strength and viability at single-cell resolution. Angew Chem Int Ed 57(1):236–240. https://doi.org/10.1002/anie.201710273
4. Zhu Z, Yang CJ (2016) Hydrogel droplet microfluidics for high-throughput single molecule/cell analysis. Acc Chem Res 50(1):22–31. https://doi.org/10.1021/acs.accounts.6b00370
5. Buettner F, Natarajan KN, Casale FP, Proserpio V, Scialdone A, Theis FJ, Teichmann SA, Marioni JC, Stegle O (2015) Computational analysis of cell-to-cell heterogeneity in single-cell RNA-sequencing data reveals hidden subpopulations of cells. Nat Biotechnol 33(2):155–160. https://doi.org/10.1038/nbt.3102
6. Qin Y, Wu L, Schneider T, Yen GS, Wang J, Xu S, Li M, Paguirigan AL, Smith JL, Radich JP (2018) A self-digitization dielectrophoretic (SD-DEP) chip for high-efficiency single-cell capture, on-demand compartmentalization, and downstream nucleic acid analysis. Angew Chem Int Ed 130(35):11548–11553. https://doi.org/10.1002/anie.201807314
7. Fritzsch FS, Dusny C, Frick O, Schmid A (2012) Single-cell analysis in biotechnology, systems biology, and biocatalysis. Annu Rev Chem Biomol Eng 3:129–155. https://doi.org/10.1146/annurev-chembioeng-062011-081056
8. Huang Q, Mao S, Khan M, Zhou L, Lin J-M (2018) Dean flow assisted cell ordering system for lipid profiling in single-cells using mass spectrometry. Chem Commun 54(21):2595–2598. https://doi.org/10.1039/c7cc09608a
9. Lan F, Demaree B, Ahmed N, Abate AR (2017) Single-cell genome sequencing at ultra-high-throughput with microfluidic droplet barcoding. Nat Biotechnol 35(7):640. https://doi.org/10.1038/nbt.3880
10. Terekhov SS, Smirnov IV, Stepanova AV, Bobik TV, Mokrushina YA, Ponomarenko NA, Belogurov AA, Rubtsova MP, Kartseva OV, Gomzikova MO, Moskovtsev AA (2017) Microfluidic droplet platform for ultrahigh-throughput single-cell screening of biodiversity. Proc Natl Acad Sci USA 114(10):201621226. https://doi.org/10.1073/pnas.1621226114
11. Wood DK, Weingeist DM, Bhatia SN, Engelward BP (2010) Single cell trapping and DNA damage analysis using microwell arrays. Proc Natl Acad Sci USA 107(22):10008–10013. https://doi.org/10.1073/pnas.1004056107
12. Cole RH, Tang S-Y, Siltanen CA, Shahi P, Zhang JQ, Poust S, Gartner ZJ, Abate AR (2017) Printed droplet microfluidics for on demand dispensing of picoliter droplets and cells. Proc Natl Acad Sci USA 114(33):8728–8733. https://doi.org/10.1073/pnas.1704020114
13. Joensson HN, Andersson Svahn H (2012) Droplet microfluidics—a tool for single-cell analysis. Angew Chem Int Ed 51(49):12176–12192. https://doi.org/10.1002/anie.201200460
14. Shang L, Cheng Y, Zhao Y (2017) Emerging droplet microfluidics. Chem Rev 117(12):7964–8040. https://doi.org/10.1021/acs.chemrev.6b00848
15. Zhang W, Li N, Koga D, Zhang Y, Zeng H, Nakajima H, Lin J-M, Uchiyama K (2018) Inkjet printing based droplet generation for integrated online digital polymerase chain reaction. Anal Che 90(8):5329–5334. https://doi.org/10.1021/acs.analchem.8b00463
16. Yusof A, Keegan H, Spillane CD, Sheils OM, Martin CM, O'Leary JJ, Zengerle R, Koltay P (2011) Inkjet-like printing of single-cells. Lab Chip 11(14):2447–2454. https://doi.org/10.1039/c1lc20176j
17. Zhong Q, Bhattacharya S, Kotsopoulos S, Olson J, Taly V, Griffiths AD, Link DR, Larson JW (2011) Multiplex digital PCR: breaking the one target per color barrier of quantitative PCR. Lab Chip 11(13):2167–2174. https://doi.org/10.1039/c1lc20126c

18. Pekin D, Skhiri Y, Baret JC, Le CD, Mazutis L, Salem CB, Millot F, El HA, Hutchison JB, Larson JW (2011) Quantitative and sensitive detection of rare mutations using droplet-based microfluidics. Lab Chip 11(13):2156–2166. https://doi.org/10.1039/c1lc20128j
19. Konry T, Dominguezvillar M, Baecherallan C, Hafler DA, Yarmush ML (2011) Droplet-based microfluidic platforms for single T cell secretion analysis of IL-10 cytokine. Biosens Bioelectron 26(5):2707–2710. https://doi.org/10.1016/j.bios.2010.09.006
20. Konry T, Golberg A, Yarmush M (2013) Live single cell functional phenotyping in droplet nano-liter reactors. Sci Rep 3(11):3179. https://doi.org/10.1038/srep03179
21. Solvas XCI, Niu X, Leeper K, Cho S, Chang SI, Edel JB, Demello AJ (2011) Fluorescence detection methods for microfluidic droplet platforms. J Vis Exp 58:3437. https://doi.org/10.3791/3437
22. Chen Q, Utech S, Chen D, Prodanovic R, Lin J-M, Weitz DA (2016) Controlled assembly of heterotypic cells in a core–shell scaffold: organ in a droplet. Lab Chip 16(8):1346–1349. https://doi.org/10.1039/C6LC00231E
23. Chen Q, Dong C, Jing W, Lin JM (2016) Flexible control of cellular encapsulation, permeability, and release in a droplet-templated bifunctional copolymer scaffold. Biomicrofluidics 10(6):064115. https://doi.org/10.1063/1.4972107
24. Christopher GF, Anna SL (2007) Microfluidic methods for generating continuous droplet streams. J Phys D Appl Phys 40(19):R319–R336(318). https://doi.org/10.1088/0022-3727/40/19/r01
25. de Menech M, Garstecki P, Jousse F, Stone HA (2008) Transition from squeezing to dripping in a microfluidic T-shaped junction. J Fluid Mech 595(595):141–161. https://doi.org/10.1017/S002211200700910X
26. Liu J, Lin J-M, Knopp D (2008) Using a circular groove surrounded inlet to generate monodisperse droplets inside a microfluidic chip in a gravity-driven manner. J Micromech Microeng 18(9):095014. https://doi.org/10.1088/0960-1317/18/9/095014
27. Haeberle S, Zengerle R, Ducrée J (2007) Centrifugal generation and manipulation of droplet emulsions. Microfluid Nanofluid 3(1):65–75. https://doi.org/10.1007/s10404-006-0106-7
28. Li H-F, Pang Y-F, Liu J-J, Lin J-M (2011) Suspending nanoliter droplet arrays for cell capture and copper ion stimulation. Sens Actuators B: Chem 155(1):415–421. https://doi.org/10.1016/j.snb.2010.12.023
29. Cramer C, Fischer P, Windhab EJ (2004) Drop formation in a co-flowing ambient fluid. Chem Eng Sci 59(15):3045–3058. https://doi.org/10.1016/j.ces.2004.04.006
30. Thorsen T, Roberts RW, Arnold FH, Quake SR (2001) Dynamic pattern formation in a vesicle-generating microfluidic device. Phys Rev Lett 86(18):4163–4166. https://doi.org/10.1103/physrevlett.86.4163
31. Basova EY, Foret F (2014) Droplet microfluidics in (bio)chemical analysis. Analyst 140(1):22–38. https://doi.org/10.1039/c4an01209g
32. Okushima S, Nisisako T, Torii T, Higuchi T (2004) Controlled production of monodisperse double emulsions by two-step droplet breakup in microfluidic devices. Langmuir 20(23):9905–9908. https://doi.org/10.1021/la0480336
33. Lin R, Fisher JS, Simon MG, Lee AP (2012) Novel on-demand droplet generation for selective fluid sample extraction. Biomicrofluidics 6(2):024103. https://doi.org/10.1063/1.3699972
34. Ding Y, i Solvas XC (2015) "V-junction": a novel structure for high-speed generation of bespoke droplet flows. Analyst 140(2):414–421. https://doi.org/10.1039/c4an01730g
35. Eggersdorfer M, Zheng W, Nawar S, Mercandetti C, Ofner A, Leibacher I, Koehler S, Weitz D (2017) Tandem emulsification for high-throughput production of double emulsions. Lab Chip 17(5):936–942. https://doi.org/10.1039/C6LC01553K
36. Chen F, Lin L, Zhang J, He Z, Uchiyama K, Lin J-M (2016) Single-cell analysis using drop-on-demand inkjet printing and probe electrospray ionization mass spectrometry. Anal Chem 88(8):4354–4360. https://doi.org/10.1021/acs.analchem.5b04749

37. Zhang W, Li N, Zeng H, Nakajima H, Lin J-M, Uchiyama K (2017) Inkjet printing based separation of mammalian cells by capillary electrophoresis. Anal Chem 89(17):8674–8677. https://doi.org/10.1021/acs.analchem.7b02624
38. Korenaga A, Chen F, Li H, Uchiyama K, Lin J-M (2017) Inkjet automated single cells and matrices printing system for matrix-assisted laser desorption/ionization mass spectrometry. Talanta 162:474–478. https://doi.org/10.1016/j.talanta.2016.10.055
39. Liu W, Mao S, Wu J, Lin J-M (2013) Development and applications of paper-based electrospray ionization-mass spectrometry for monitoring of sequentially generated droplets. Analyst 138(7):2163–2170. https://doi.org/10.1039/C3AN36404F
40. Liu W, Wang N, Lin X, Ma Y, Lin J-M (2014) Interfacing microsampling droplets and mass spectrometry by paper spray ionization for online chemical monitoring of cell culture. Anal Chem 86(14):7128–7134. https://doi.org/10.1021/ac501678q
41. Link DR, Grasland-Mongrain E, Duri A, Sarrazin F, Cheng Z, Cristobal G, Marquez M, Weitz DA (2006) Electric control of droplets in microfluidic devices. Angew Chem Int Ed 45(16):2556–2560. https://doi.org/10.1002/anie.200503540
42. Liu J, Tan S-H, Yap YF, Ng MY, Nguyen N-T (2011) Numerical and experimental investigations of the formation process of ferrofluid droplets. Microfluid Nanofluid 11 (2):177–187. https://doi.org/10.1007/s10404-011-0784-7
43. Nguyen NT, Ting TH, Yap YF, Wong TN, Chai CK, Ong WL, Zhou J, Tan SH, Yobas L (2007) Thermally mediated droplet formation in microchannels. Appl Phys Lett 91(8): s10404
44. Xiong S, Chin LK, Ando K, Tandiono T, Liu AQ, Ohl CD (2015) Droplet generation via a single bubble transformation in a nanofluidic channel. Lab Chip 15(6):1451–1457. https://doi.org/10.1039/c4lc01184h
45. Park SY, Wu TH, Chen Y, Teitell MA, Chiou PY (2011) High-speed droplet generation on demand driven by pulse laser-induced cavitation. Lab Chip 11(6):1010–1012. https://doi.org/10.1039/c0lc00555j
46. Huebner A, Srisa-Art M, Holt D, Abell C, Hollfelder F, Demello AJ, Edel JB (2007) Quantitative detection of protein expression in single cells using droplet microfluidics. Chem Commun 28(12):1218–1220. https://doi.org/10.1039/b618570c
47. Collins DJ, Neild A, Demello A, Liu AQ, Ai Y (2015) The Poisson distribution and beyond: methods for microfluidic droplet production and single cell encapsulation. Lab Chip 15 (17):3439–3459. https://doi.org/10.1039/c5lc00614g
48. Chabert M, Viovy JL (2008) Microfluidic high-throughput encapsulation and hydrodynamic self-sorting of single cells. Proc Natl Acad Sci USA 105(9):3191–3196. https://doi.org/10.1073/pnas.0708321105
49. Jing T, Ramji R, Warkiani ME, Han J, Lim CT, Chen CH (2015) Jetting microfluidics with size-sorting capability for single-cell protease detection. Biosens Bioelectron 66:19–23. https://doi.org/10.1016/j.bios.2014.11.001
50. Edd JF, Di Carlo D, Humphry KJ, Köster S, Irimia D, Weitz DA, Toner M (2008) Controlled encapsulation of single-cells into monodisperse picolitre drops. Lab Chip 8 (8):1262–1264. https://doi.org/10.1039/b805456h
51. Kemna EW, Schoeman RM, Wolbers F, Vermes I, Weitz DA, Van Den Berg A (2012) High-yield cell ordering and deterministic cell-in-droplet encapsulation using Dean flow in a curved microchannel. Lab Chip 12(16):2881–2887. https://doi.org/10.1039/c2lc00013j
52. Ramji R, Wang M, Bhagat AAS, Weng DTS, Thakor NV, Lim CT, Chen CH (2014) Single cell kinase signaling assay using pinched flow coupled droplet microfluidics. Biomicrofluidics 8(3):47–53. https://doi.org/10.1063/1.4878635
53. Novo P, Dell'Aica M, Janasek D, Zahedi RP (2016) High spatial and temporal resolution cell manipulation techniques in microchannels. Analyst 141(6):1888–1905. https://doi.org/10.1039/C6AN00027D
54. Dudani JS, Gossett DR, Tse HT, Di CD (2013) Pinched-flow hydrodynamic stretching of single-cells. Lab Chip 13(18):3728–3734. https://doi.org/10.1039/c3lc50649e

55. Mcgrath J, Jimenez M, Bridle H (2014) Deterministic lateral displacement for particle separation: a review. Lab Chip 14(21):4139–4158. https://doi.org/10.1039/C4LC00939H
56. Cheng Q, Huang H, Chen L, Li X, Ge Z, Chen T, Yang Z, Sun L (2014) Dielectrophoresis for bioparticle manipulation. Int J Mol Sci 15(10):18281. https://doi.org/10.3390/ijms151018281
57. Zhang H, Liu KK (2008) Optical tweezers for single cells. J R Soc Interface 5(24):671–690. https://doi.org/10.1098/rsif.2008.0052
58. Lim B, Reddy V, Hu XH, Kim KW, Jadhav M, Abedini-Nassab R, Noh YW, Yong TL, Yellen BB, Kim CG (2014) Magnetophoretic circuits for digital control of single particles and cells. Nat Commun 5:3846. https://doi.org/10.1038/ncomms4846
59. Ahmed D, Ozcelik A, Bojanala N, Nama N, Upadhyay A, Chen Y, Hannarose W, Huang TJ (2016) Rotational manipulation of single cells and organisms using acoustic waves. Nat Commun 7:11085. https://doi.org/10.1038/ncomms11085
60. Yarmush ML, King KR (2009) Living-cell microarrays. Annu Rev Biomed Eng 11(1):235. https://doi.org/10.1146/annurev.bioeng.10.061807.160502
61. Jonczyk R, Kurth T, Lavrentieva A, Walter JG, Scheper T, Stahl F (2016) Living cell microarrays: an overview of concepts. Microarrays 5(2):11. https://doi.org/10.3390/microarrays5020011
62. Lin L, Chu YS, Thiery JP, Lim CT, Rodriguez I (2013) Microfluidic cell trap array for controlled positioning of single cells on adhesive micropatterns. Lab Chip 13(4):714. https://doi.org/10.1039/c2lc41070b
63. Sarioglu AF, Aceto N, Kojic N, Donaldson MC, Zeinali M, Hamza B, Engstrom A, Zhu H, Sundaresan TK, Miyamoto DT (2015) A microfluidic device for label-free, physical capture of circulating tumor cell clusters. Nat Methods 12(7):685–691. https://doi.org/10.1038/nmeth.3404
64. Lecault V, Vaninsberghe M, Sekulovic S, Knapp DJHF, Wohrer S, Bowden W, Viel F, Mclaughlin T, Jarandehei A, Miller M (2011) High-throughput analysis of single hematopoietic stem cell proliferation in microfluidic cell culture arrays. Nat Methods 8(7):581. https://doi.org/10.1038/nmeth.1614
65. Voldman J (2006) Electrical forces for microscale cell manipulation. Annu Rev Biomed Eng 8(8):425–454. https://doi.org/10.1146/annurev.bioeng.8.061505.095739
66. Yasukawa T, Nagamine K, Horiguchi Y, Shiku H, Koide M, Itayama T, Shiraishi F, Matsue T (2008) Electrophoretic cell manipulation and electrochemical gene-function analysis based on a yeast two-hybrid system in a microfluidic device. Anal Chem 80(10):3722–3727. https://doi.org/10.1021/ac800143t
67. Park K, Suk HJ, Akin D, Bashir R (2009) Dielectrophoresis-based cell manipulation using electrodes on a reusable printed circuit board. Lab Chip 9(15):2224–2229. https://doi.org/10.1039/b904328d
68. Glawdel T, Ren CL (2009) Electro-osmotic flow control for living cell analysis in microfluidic PDMS chips. Mech Res Commun 36(1):75–81. https://doi.org/10.1016/j.mechrescom.2008.06.015
69. Mehrishi JN, Bauer J (2015) Electrophoresis of cells and the biological relevance of surface charge. Electrophoresis 23(13):1984–1994. https://doi.org/10.1002/1522-2683(200207)23:13%3c1984:AID-ELPS1984%3e3.0.CO;2-U
70. Wyatt Shields Iv C, Reyes CD, López GP (2015) Microfluidic cell sorting: a review of the advances in the separation of cells from debulking to rare cell isolation. Lab Chip 15(5):1230–1249. https://doi.org/10.1039/C4LC01246A
71. Takahashi K, Hattori A, Suzuki I, Ichiki T, Yasuda K (2004) Non-destructive on-chip cell sorting system with real-time microscopic image processing. J Nanobiotechnol 2(1):5. https://doi.org/10.1186/1477-3155-2-5
72. Guo F, Ji XH, Liu K, He RX, Zhao LB, Guo ZX, Liu W, Guo SS, Zhao XZ (2010) Droplet electric separator microfluidic device for cell sorting. Appl Phys Lett 96(19):1392. https://doi.org/10.1063/1.3360812

73. Plouffe BD, Murthy SK, Lewis LH (2015) Fundamentals and application of magnetic particles in cell isolation and enrichment: a review. Rep Prog Phys 78(1):016601. https://doi.org/10.1088/0034-4885/78/1/016601
74. Pohl HA (1951) The motion and precipitation of suspensoids in divergent electric fields. J Appl Phys 22(7):869–871. https://doi.org/10.1063/1.1700065
75. Gascoyne PR, Vykoukal J (2015) Particle separation by dielectrophoresis. Electrophoresis 23(13):1973–1983. https://doi.org/10.1002/1522-2683(200207)23:13%3c1973::AID-ELPS1973%3e3.0.CO;2-1
76. Chuang CH, Wu YT (2012) Dielectrophoretic chip with multilayer electrodes and micro-cavity array for trapping and programmably releasing single cells. Biomed Microdevices 14(2):271–278. https://doi.org/10.1007/s10544-011-9603-x
77. Thomas RS, Morgan H, Green NG (2009) Negative DEP traps for single cell immobilisation. Lab Chip 9(11):1534–1540. https://doi.org/10.1039/B819267G
78. Jang L-S, Huang P-H, Lan K-C (2009) Single-cell trapping utilizing negative dielectrophoretic quadrupole and microwell electrodes. Biosens Bioelectron 24(12):3637–3644. https://doi.org/10.1016/j.bios.2009.05.027
79. Park H, Kim D, Yun KS (2010) Single-cell manipulation on microfluidic chip by dielectrophoretic actuation and impedance detection. Sens Actuators B-Chem 150(1):167–173. https://doi.org/10.1016/j.snb.2010.07.020
80. Kim SH, Yamamoto T, Fourmy D, Fujii T (2011) Electroactive microwell arrays for highly efficient single-cell trapping and analysis. Small 7(22):3239–3247. https://doi.org/10.1002/smll.201101028
81. Dittrich PS, Schwille P (2003) An integrated microfluidic system for reaction, high-sensitivity detection, and sorting of fluorescent cells and particles. Anal Chem 75(21):5767–5774. https://doi.org/10.1021/ac034568c
82. Ashkin A (1970) Acceleration and trapping of particles by radiation pressure. Phys Rev Lett 24(4):156. https://doi.org/10.1103/physrevlett.24.156
83. Ashkin A, Dziedzic JM, Bjorkholm J, Chu S (1986) Observation of a single-beam gradient force optical trap for dielectric particles. Opt Lett 11(5):288–290. https://doi.org/10.1364/OL.11.000288
84. Hosic S, Murthy SK, Koppes AN (2016) Microfluidic sample preparation for single cell analysis. Anal Chem 88(1):354–380. https://doi.org/10.1021/acs.analchem.5b04077
85. Jonáš A, Zemanek P (2008) Light at work: the use of optical forces for particle manipulation, sorting, and analysis. Electrophoresis 29(24):4813–4851. https://doi.org/10.1002/elps.200800484
86. Moffitt JR, Chemla YR, Smith SB, Bustamante C (2008) Recent advances in optical tweezers. Annu Rev Biochem 77:205–228. https://doi.org/10.1146/annurev.biochem.77.043007.090225
87. Bellini N, Vishnubhatla KC, Bragheri F, Ferrara L, Minzioni P, Ramponi R, Cristiani I, Osellame R (2010) Femtosecond laser fabricated monolithic chip for optical trapping and stretching of single cells. Opt Express 18(5):4679–4688. https://doi.org/10.1364/OE.18.004679
88. Kim SB, Yoon SY, Sung HJ, Kim SS (2008) Cross-type optical particle separation in a microchannel. Anal Chem 80(7):2628–2630. https://doi.org/10.1021/ac8000918
89. Kovac J, Voldman J (2007) Intuitive, image-based cell sorting using optofluidic cell sorting. Anal Chem 79(24):9321–9330. https://doi.org/10.1021/ac071366y
90. Wang C, Ye M, Cheng L, Li R, Zhu W, Shi Z, Fan C, He J, Liu J, Liu Z (2015) Simultaneous isolation and detection of circulating tumor cells with a microfluidic silicon-nanowire-array integrated with magnetic upconversion nanoprobes. Biomaterials 54:55–62. https://doi.org/10.1016/j.biomaterials.2015.03.004
91. Liu J, Shi J, Jiang L, Zhang F, Wang L, Yamamoto S, Takano M, Chang M, Zhang H, Chen Y (2012) Segmented magnetic nanofibers for single cell manipulation. Appl Surf Sci 258(19):7530–7535. https://doi.org/10.1016/j.apsusc.2012.04.077

92. Burguillos MA, Magnusson C, Nordin M, Lenshof A, Augustsson P, Hansson MJ, Elmer E, Lilja H, Brundin P, Laurell T (2013) Microchannel acoustophoresis does not impact survival or function of microglia, leukocytes or tumor cells. PLoS One 8(5):e64233. https://doi.org/10.1371/journal.pone.0064233
93. Grenvall C, Magnusson C, Lilja H, Laurell T (2015) Concurrent isolation of lymphocytes and granulocytes using prefocused free flow acoustophoresis. Anal Chem 87(11):5596. https://doi.org/10.1021/acs.analchem.5b00370
94. Li S, Ding X, Guo F, Chen Y, Lapsley MI, Lin SCS, Wang L, Mccoy JP, Cameron CE, Huang TJ (2013) An on-chip, multichannel droplet sorter using standing surface acoustic waves. Anal Chem 85(11):5468–5474. https://doi.org/10.1021/ac400548d
95. Schmid L, Weitz DA, Franke T (2014) Sorting drops and cells with acoustics: acoustic microfluidic fluorescence-activated cell sorter. Lab Chip 14(19):3710–3718. https://doi.org/10.1039/c4lc00588k
96. And JRR, Folch A (2005) Large-scale single-cell trapping and imaging using microwell arrays. Anal Chem 77(17):5628–5634. https://doi.org/10.1021/ac0505977
97. Carlo DD, Wu LY, Lee LP (2006) Dynamic single cell culture array. Lab Chip 6(11):1445–1449. https://doi.org/10.1039/b605937f
98. Chen J, Chen D, Yuan T, Chen X, Zhu J, Morschhauser A, Nestler J, Otto T, Gessner T (2014) Microfluidic chips for cells capture using 3-D hydrodynamic structure array. Microsyst Technol 20(3):485–491. https://doi.org/10.1007/s00542-013-1933-6
99. Chung J, Kim YJ, Yoon E (2011) Highly-efficient single-cell capture in microfluidic array chips using differential hydrodynamic guiding structures. Appl Phys Lett 98(12):123701. https://doi.org/10.1063/1.3565236
100. Fröhlich J, König H (2000) New techniques for isolation of single prokaryotic cells 1. FEMS Microbiol Rev 24(5):567–572. https://doi.org/10.1111/j.1574-6976.2000.tb00558.x
101. Anis Y, Houkal J, Holl M, Johnson R, Meldrum D (2011) Diaphragm pico-liter pump for single-cell manipulation. Biomed Microdevices 13(4):651–659. https://doi.org/10.1007/s10544-011-9535-5
102. Kim BC, Moraes C, Huang J, Matsuoka T, Thouless MD, Takayama S (2015) Fracture-based fabrication of normally closed, adjustable, and fully reversible microscale fluidic channels. Small 10(19):4020–4029. https://doi.org/10.1002/smll.201400147
103. Hoefemann H, Wadle S, Bakhtina N, Kondrashov V, Wangler N, Zengerle R (2012) Sorting and lysis of single cells by BubbleJet technology. Sens Actuators B-Chem 168(12):442–445. https://doi.org/10.1016/j.snb.2012.04.005
104. Gong Y, Ogunniyi AO, Love JC (2010) Massively parallel detection of gene expression in single cells using subnanolitre wells. Lab Chip 10(18):2334–2337. https://doi.org/10.1039/c004847j
105. Liu ET, Lauffenburger DA (2009) Systems biomedicine: concepts and perspectives. Academic Press, Salt Lake
106. Shi Q, Qin L, Wei W, Geng F, Fan R, Shin YS, Guo D, Hood L, Mischel PS, Heath JR (2012) Single-cell proteomic chip for profiling intracellular signaling pathways in single tumor cells. Proc Natl Acad Sci USA 109(2):419–424. https://doi.org/10.1073/pnas.1110865109
107. White AK, Heyries KA, Doolin C, Vaninsberghe M, Hansen CL (2013) High-throughput microfluidic single-cell digital polymerase chain reaction. Anal Chem 85(15):7182–7190. https://doi.org/10.1021/ac400896j
108. Treutlein B, Brownfield DG, Wu AR, Neff NF, Mantalas GL, Espinoza FH, Desai TJ, Krasnow MA, Quake SR (2014) Reconstructing lineage hierarchies of the distal lung epithelium using single-cell RNA-seq. Nature 509(7500):371–375. https://doi.org/10.1038/nature13173
109. Streets AM, Zhang X, Cao C, Pang Y, Wu X, Xiong L, Yang L, Fu Y, Zhao L, Tang F (2014) Microfluidic single-cell whole-transcriptome sequencing. Proc Natl Acad Sci USA 111(19):7048. https://doi.org/10.1073/pnas.1402030111

110. Fan HC, Wang J, Potanina A, Quake SR (2011) Whole-genome molecular haplotyping of single cells. Nat Biotechnol 29(1):51–57. https://doi.org/10.1038/nbt.1739
111. Sun H, Olsen T, Zhu J, Tao J, Ponnaiya B, Amundson SA, Brenner DJ, Lin Q (2014) A Bead-based microfluidic approach to integrated single-cell gene expression analysis by quantitative RT-PCR. RSC Adv 5(7):4886–4893. https://doi.org/10.1039/C4RA13356K
112. DeKosky BJ, Kojima T, Rodin A, Charab W, Ippolito GC, Ellington AD, Georgiou G (2015) In-depth determination and analysis of the human paired heavy-and light-chain antibody repertoire. Nat Med 21(1):86. https://doi.org/10.1007/978-3-319-58518-5_3
113. Macosko E, Basu A, Satija R, Nemesh J, Shekhar K, Goldman M, Tirosh I, Bialas A, Kamitaki N, Martersteck E (2015) Highly parallel genome-wide expression profiling of individual cells using nanoliter droplets. Cell 161(5):1202–1214. https://doi.org/10.1016/j.cell.2015.05.002
114. Klein Allon M, Mazutis L, Akartuna I, Tallapragada N, Veres A, Li V, Peshkin L, Weitz David A, Kirschner Marc W (2015) Droplet barcoding for single-cell transcriptomics applied to embryonic stem cells. Cell 161(5):1187–1201. https://doi.org/10.1016/j.cell.2015.04.044
115. Rival A, Jary D, Delattre C, Fouillet Y, Castellan G, Bellemincomte A, Gidrol X (2014) An EWOD-based microfluidic chip for single-cell isolation, mRNA purification and subsequent multiplex qPCR. Lab Chip 14(19):3739–3749. https://doi.org/10.1039/C4LC00592A
116. Zinchenko A, Devenish SR, Kintses B, Colin PY, Fischlechner M, Hollfelder F (2014) One in a million: flow cytometric sorting of single cell-lysate assays in monodisperse picolitre double emulsion droplets for directed evolution. Anal Chem 86(5):2526–2533. https://doi.org/10.1021/ac403585p
117. Sarkar A, Kolitz S, Lauffenburger DA, Han J (2014) Microfluidic probe for single-cell lysis and analysis in adherent tissue culture. Nat Commun 5(5):3421. https://doi.org/10.1038/ncomms4421
118. Tsong TY (1991) Electroporation of cell membranes. Biophys J 60(2):297–306. https://doi.org/10.3109/07388559609147426
119. Sersa G, Miklavcic D, Cemazar M, Rudolf Z, Pucihar G, Snoj M (2008) Electrochemotherapy in treatment of tumours. Eur J Surg Oncol 34(2):232–240. https://doi.org/10.1016/j.ejso.2007.05.016
120. Lee SW, Tai YC (1999) A micro cell lysis device. Sens Actuator A-Phys 73(1–2):74–79. https://doi.org/10.1016/S0924-4247(98)00257-X
121. Lu H, Schmidt MA, Jensen KF (2004) A microfluidic electroporation device for cell lysis. Lab Chip 5(1):23–29. https://doi.org/10.1039/B406205A
122. Chao-Wang Y, Jia-Ling H, Chyung A (2012) Development of an integrated chip for automatic tracking and positioning manipulation for single cell lysis. Sensors 12(3):2400–2413. https://doi.org/10.3390/s120302400